Combined Gradient Projection / Single Component Artificial Force Induced Reaction (GP/SC-AFIR) Method for an Efficient Search of Minimum Energy Conical Intersection (MECI) Geometries

Yu Harabuchi,[a,b,*] Tetsuya Taketsugu,[a] and Satoshi Maeda[a,*]

[a]Department of Chemistry, Faculty of Science, Hokkaido University, Sapporo 060-0810, Japan.

[b]JST, PRESTO, 4-1-8 Honcho, Kawaguchi, Saitama, 332-0012, Japan

Abstract: We report a new approach to search for structures of minimum energy conical intersection (MECIs) automatically. Gradient projection (GP) method and single component artificial force induced reaction (SC-AFIR) method were combined in the present approach. As case studies, MECIs of benzene and naphthalene between their ground and first excited singlet electronic states (S_0/S_1-MECIs) were explored. All S_0/S_1-MECIs reported previously were obtained automatically. Furthermore, the number of force calculations was reduced compared to the one required in the previous search.

Improved convergence in a step in which various geometrical displacements are induced by SC-AFIR would contribute to the cost reduction.

Graphical abstract

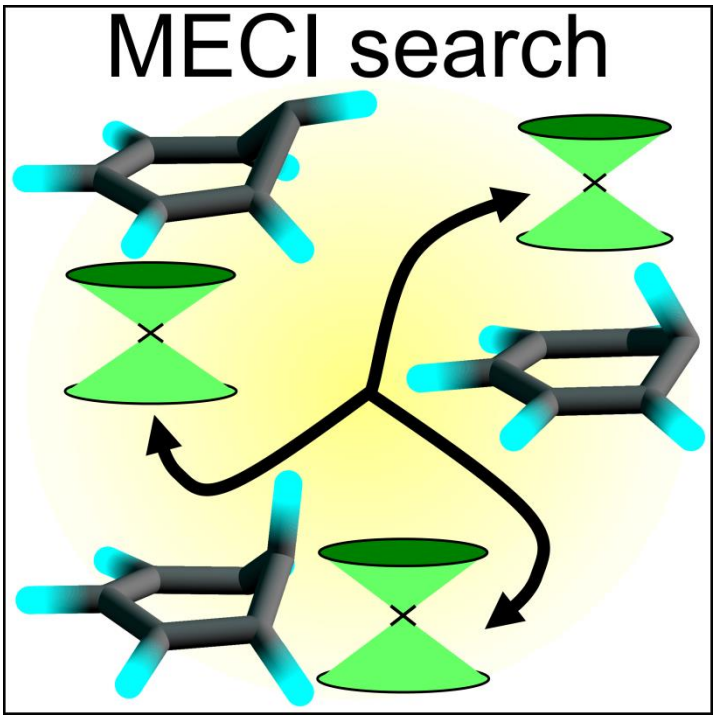

Keywords

Conical intersection, Artificial force induced reaction, Gradient projection, Global reaction route mapping, Benzene, Naphthalene

Highlights

1. We propose an efficient method to search for MECI structures automatically.

2. The gradient projection method was combined with the SC-AFIR method.

3. Numerical tests were conducted on benzene and naphthalene.

4. The new approach generated all previously reported MECIs automatically.

5. The new approach was shown to be more efficient than the previous method.

1. Introduction

It has been widely recognized that conical intersection (CI) plays an important role in photo-decay processes through a non-radiative transition. CI is a $3N - 8$ dimensional hyperspace in which two adiabatic potentials of different electronic states with the same spin and space symmetry are degenerate. A number of photoreactions have been discussed based on the geometrical deformation of molecules caused by a molecular motion leading to a CI region [1-6]. The minimum energy point within a CI hyperspace, which has been called as minimum energy conical intersection (MECI), has been optimized as an energetically most favorable geometry. There are several methods to optimize a MECI geometry [7-15]. Molecules decay to the lower electronic state in higher-energy regions of the CI hyperspace in the actual dynamics, and characterization of higher-energy CI regions have also been made [16-18]. Automated methods have also been developed for systematic exploration of MECI geometries [19-22].

Such an automated MECI search has been made based on the seam model function (SMF) approach, in which an automated search of local minima is made on a

model function [23]. The model function consists of two terms, i.e., the mean energy of target states and a penalty function. The penalty is large when the energy gap between target states is large. The model function has local minima near MECIs, and approximate MECI geometries can therefore be obtained by exploring local minima on the model function. Three automated reaction path search methods, i.e., anharmonic downward distortion following (ADDF) [24-26], multi component artificial force induced reaction (MC-AFIR) [27], and single component (SC)-AFIR [28], have been employed to search for local minima on the model function [20-22]. Especially, the SMF/SC-AFIR approach has enabled automated search of MECI geometries in systems including more than 30 atoms routinely using a laboratory size computer cluster [22].

Improving efficiency of the automated search for MECIs by the SC-AFIR method is the subject of this study. In the SMF method, a penalty function is used to find approximate MECI geometries as local minima. However, it is known in optimization of an MECI geometry that convergence of geometry optimization is slow when a penalty function approach is employed [12]. This discussion suggests that the automated search can be accelerated by combining the SC-AFIR method with a method which does not use penalty function. In this study, the gradient projection (GP) method [9,14], which has been used as one of MECI optimization methods, has therefore been

combined with the SC-AFIR method. The GP/SC-AFIR approach was shown to be more efficient than the previous SMF/SC-AFIR method, because of significant improvement in convergence in the stage to induce a systematic geometrical deformation by the SC-AFIR method.

2. Methodology

2-1. Single component artificial force induced reaction method

The AFIR method finds the other minima starting from a minimum by minimizing an AFIR function, $F^{\mathrm{AFIR}}(\mathbf{Q})$. The AFIR function which adds an artificial force between a given fragment pair, A and B, is defined by **Equation (1)**.

$$F^{\mathrm{AFIR}}(\mathbf{Q}) = E(\mathbf{Q}) + \rho\alpha \frac{\sum_{i\in A}\sum_{j\in B} \omega_{ij} r_{ij}}{\sum_{i\in A}\sum_{j\in B} \omega_{ij}} \qquad (1)$$

$E(\mathbf{Q})$ is the adiabatic potential energy surface (PES) of coordinate **Q**, and the second term corresponds to the artificial force term. A constant parameter α determines the strength of the force, and ρ is either 1.0 or −1.0 to push fragments together or to pull them apart, respectively. The value of α is given by **Equation (2)**.

$$\alpha = \frac{\gamma}{\left[2^{-\frac{1}{6}} - \left(1+\sqrt{1+\frac{\gamma}{\varepsilon}}\right)^{-\frac{1}{6}}\right] R_0} \qquad (2)$$

R_0 and ε are the standard Ar-Ar parameters of Lennard-Jones potential, i.e., R_0 = 3.8164 Å and ε = 1.0061 kJ/mol. The constant parameter γ is the model collision energy parameter and is defined by users, where γ provides an approximate upper limit of the barrier height which can be overcome by a minimization of the AFIR function. In **Equation (1)**, r_{ij} is a distance between an atom pair, i and j, and ω_{ij} is the weight function defined in **Equation (3)**.

$$\omega_{ij} = \left[\frac{\left(R_i + R_j\right)}{r_{ij}} \right]^p \qquad (3)$$

R_i is the covalent radius for atom i, and p is set to the standard value 6.0. Details for the AFIR function are discussed in the previous papers [27,29]. The path of minimization of AFIR function is called as AFIR-path.

Along an AFIR-path, approximate minima and transition states are obtained as local energy minima and maxima, respectively. In this study, the minimum-only (MIN-only) algorithm [29] in which local maxima of an energy variation along the AFIR-path are ignored, is employed. The procedure, which is applied to a given fragment pair, consists of the following two steps: (1) minimization of $F^{\mathrm{AFIR}}(\mathbf{Q})$ to obtain an AFIR-path, and (2) minimization of $E(\mathbf{Q})$ starting from all approximate minima which are obtained as local minima of an energy variation along the AFIR-path. The second step gives local minima on $E(\mathbf{Q})$, and a number of local minima on $E(\mathbf{Q})$

can be obtained by applying this procedure to all possible fragment pairs. An algorithm to generate fragment pairs systematically is described in our previous papers [28,29].

2-2. Gradient projection method

The GP method is one of MECI optimization methods [9,14]. It uses a composed force vector $\mathbf{g}^{GP}$ given in **Equation (4)** to optimize an MECI geometry between two states X and Y.

$$\mathbf{g}^{GP}(\mathbf{Q}) = 2\left(E^{X}(\mathbf{Q}) - E^{Y}(\mathbf{Q})\right)\mathbf{v}^{DGV} + \mathbf{P}\frac{1}{2}\left(\frac{dE^{X}(\mathbf{Q})}{d\mathbf{Q}} + \frac{dE^{Y}(\mathbf{Q})}{d\mathbf{Q}}\right) \quad (4)$$

The matrix **P** is defined as below.

$$\mathbf{P} = \mathbf{1} - \mathbf{v}^{DGV}\left(\mathbf{v}^{DGV}\right)^{T} - \mathbf{v}^{DCV}\left(\mathbf{v}^{DCV}\right)^{T} \quad (5)$$

$E^{X}(\mathbf{Q})$ and $E^{Y}(\mathbf{Q})$ are the adiabatic PESs of coordinates **Q** for states X and Y, respectively. $dE^{X}(\mathbf{Q})/d\mathbf{Q}$ and $dE^{Y}(\mathbf{Q})/d\mathbf{Q}$ correspond to the gradient vectors of $E^{X}(\mathbf{Q})$ and $E^{Y}(\mathbf{Q})$, respectively. $\mathbf{v}^{DGV}$ is an unit vector of the difference gradient vector (DGV) which can be easily computed from gradient vectors of the two adiabatic PESs, and $\mathbf{v}^{DCV}$ is an unit vector parallel to the derivative coupling vector (DCV).

As shown in **Equation (5)**, the GP method requires a plane composed of two vectors $\mathbf{v}^{DGV}$ and $\mathbf{v}^{DCV}$. This plane is called branching plane (BP). In this study, the BP update (BPU) approach was used to obtain the BP at each geometry, and a unit vector

perpendicular to $\mathbf{v}^{DGV}$ in the BP is used in **Equation (5)** instead of $\mathbf{v}^{DCV}$ [15]. The BPU approach can estimate a BP using only gradients for adiabatic PESs calculated at the present and previous optimization steps. In the BPU, the BP is estimated assuming the first-order expansion of the two diabatic PESs. The equation to obtain the first-order BP using gradients of the two adiabatic PESs calculated at the present and previous optimization steps and its derivation are described in our previous papers [15,23]. By using the BPU method, calculation of DCV can be avoided.

2-3. GP/SC-AFIR method

In the GP/SC-AFIR method for two target states X and Y, geometry optimization by the GP method is applied to a pair of AFIR functions, $F^{\text{AFIR-X}}(\mathbf{Q})$ and $F^{\text{AFIR-Y}}(\mathbf{Q})$, in which adiabatic PESs, $E^{\text{X}}(\mathbf{Q})$ and $E^{\text{Y}}(\mathbf{Q})$, are used as $E(\mathbf{Q})$ in **Equation (1)**, respectively. It is noted that $E^{\text{X}}(\mathbf{Q}) - E^{\text{Y}}(\mathbf{Q}) = F^{\text{AFIR-X}}(\mathbf{Q}) - F^{\text{AFIR-Y}}(\mathbf{Q})$, since the force term in **Equation (1)** does not depend on electronic state.

In this study, a gradient vector $\mathbf{g}^{\text{GP/AFIR}}$ in **Equation (6)** is introduced.

$$\mathbf{g}^{\text{GP/AFIR}}(\mathbf{Q}) = 2\left(F^{\text{AFIR-X}}(\mathbf{Q}) - F^{\text{AFIR-Y}}(\mathbf{Q})\right)\mathbf{v}^{\text{DGV}} + \mathbf{P}\frac{1}{2}\left(\frac{dF^{\text{AFIR-X}}(\mathbf{Q})}{d\mathbf{Q}} + \frac{dF^{\text{AFIR-Y}}(\mathbf{Q})}{d\mathbf{Q}}\right) \quad (6)$$

A geometry optimization using $\mathbf{g}^{\text{GP/AFIR}}$ as a gradient vector converges to a local

minimum of $\{F^{\mathrm{AFIR\text{-}X}}(\mathbf{Q}) + F^{\mathrm{AFIR\text{-}Y}}(\mathbf{Q})\} / 2$ within the hyperspace in which $F^{\mathrm{AFIR\text{-}X}}(\mathbf{Q})$ and $F^{\mathrm{AFIR\text{-}Y}}(\mathbf{Q})$ are degenerate. As noted above, such a hyperspace exactly corresponds to the CI of two states X and Y, because $E^{\mathrm{X}}(\mathbf{Q}) - E^{\mathrm{Y}}(\mathbf{Q}) = F^{\mathrm{AFIR\text{-}X}}(\mathbf{Q}) - F^{\mathrm{AFIR\text{-}Y}}(\mathbf{Q})$. The force term in $F^{\mathrm{AFIR\text{-}X}}(\mathbf{Q})$ and $F^{\mathrm{AFIR\text{-}Y}}(\mathbf{Q})$ let the geometry optimization converge to various geometries depending on the choice of fragment pair to which the artificial force is applied.

A geometry optimization with $\mathbf{g}^{\mathrm{GP/AFIR}}$ gives a GP/AFIR-path, along which approximate MECI structures can be obtained as local minima of a variation of either $\{E^{\mathrm{X}}(\mathbf{Q}) + E^{\mathrm{Y}}(\mathbf{Q})\} / 2$ or the model function of **Equation (7)**.

$$F^{SMF}(\mathbf{Q}) = \frac{1}{2}\left(E^{X}(\mathbf{Q}) + E^{Y}(\mathbf{Q})\right) + \frac{\left(E^{X}(\mathbf{Q}) - E^{Y}(\mathbf{Q})\right)^{2}}{\beta} \quad \ldots(7)$$

A variation of $\{E^{\mathrm{X}}(\mathbf{Q}) + E^{\mathrm{Y}}(\mathbf{Q})\} / 2$ may have local minima not only near MECI structures but also around a local minimum of either $E^{\mathrm{X}}(\mathbf{Q})$ or $E^{\mathrm{Y}}(\mathbf{Q})$ at which the energy gap $E^{\mathrm{X}}(\mathbf{Q}) - E^{\mathrm{Y}}(\mathbf{Q})$ is not small. On the other hand, the function of **Equation (7)**, which is identical to the model function used in the SMF approach [19], has local minima only in a region in which the energy gap is small. Therefore, in this study, local minima of a variation of the model function defined in **Equation (7)** along the GP/AFIR-path are further optimized by the standard GP method to obtain *true* MECI structures. The parameter β is set to the standard value in the SMF approach, β = 30

kJ/mol [19]. It should be noted that the penalty function of **Equation (7)** is used only to find guesses of MECI structures along a GP/AFIR-path, and it does not affect the convergence of geometry optimizations using $\mathbf{g}^{\mathrm{GP/AFIR}}$.

The flow of the GP/SC-AFIR method is summarized as follows:

(a) Generate fragment pairs at a given initial structure by the algorithm reported previously [28,29].

(b) Do a geometry optimization with $\mathbf{g}^{\mathrm{GP/AFIR}}$ for one of fragment pairs defined in the step (a).

(c) Do MECI optimizations starting from all local minima of a variation of the model function denoted in **Equation (7)** along the GP/AFIR-path obtained in the step (b).

(d) Exit if steps (b) and (c) were applied to all fragment pairs generated in the step (a).

(e) Return to the step (b) and continue the search.

We note that all MECI structures obtained in this procedure are *true* MECI structures of a given computational level that are optimized without the artificial force. In this study, the matrix **P** in **Equations (5)** and **(6)** were obtained by the BPU approach [15].The search is done automatically just by running the GRRM program with a single input file in which only a single geometry, i.e., the FC geometry, is given.

The GP method itself has been used not only to optimize MECI structures but

also to optimize structures of minimum energy seam of crossing (MESX) between two different spin states [9,14]. The present approach can also be applied to the search for MESX structures. In either the automated search of MESX structures or the optimization of an MESX structure, the projection matrix **P** which is composed of the first two terms of eq. (5), is adopted.

3. Computational details

MECI structures between the ground and first excited singlet electronic states (S_0/S_1-MECIs) for benzene and naphthalene were searched by using the GP/SC-AFIR method. The collision energy parameter γ in **Equation (3)** was set to 100 kJ/mol. In the previous reports [29,30], S_0/S_1-MECIs of benzene and naphthalene were explored by using SMF/SC-AFIR method with two different γ values, i.e., γ = 100 and 200 kJ/mol. These calculations showed that γ = 100 kJ/mol was enough to obtain all important MECIs in the Franck-Condon (FC) region. As shown below, γ = 100 kJ/mol was enough to obtain these MECIs in the FC region also in the search by the present GP/SC-AFIR method [29,30]. The obtained S_0/S_1-MECIs and the number of gradient calculations required in the searches were compared with those in the previous studies [29,30]. The present test calculations were made with the spin-flip time-dependent density functional

theory (SF-TDDFT) [31-33]. The BHHLYP functional [34,35] was used in combination with the 6-31G* basis set. Benchmark calculations showed that the most successful functionals to calculate the vertical excitation energy were those including 50%-60% Hartree-Fock exchange [36], for the collinear SF-TDDFT implemented in the GAMESS program. In a case study of stilbene, it was shown that geometries and relative energies of MECIs by SF-TDDFT with BHHLYP were consistent with those by XMCQDPT2 calculations [37,38]. The basis set dependence in geometries and relative energies of MECIs in SF-TDDFT calculations with BHHLYP was also shown to be small [39]. These knowledges would justify use of SF-TDDFT with BHHLYP and 6-31G* in an efficient test of a newly developed structure search method. SF-TDDFT gradients were computed by GAMESS program package [40]. GP/SC-AFIR search was performed by using a developmental version of GRRM program [41].

4. Results and discussions

4-1. Benzene

S_0/S_1-MECI geometries of benzene are shown in **Figure 2**. S_0/S_1-MECIs obtained by GP/SC-AFIR are indicated by ‘a’, and those obtained by SMF/SC-AFIR using the same collision energy parameter, γ = 100 kJ/mol, in the previous study are indicated by ‘b’ [30]. MECIs caused by a molecular motion accompanying a bond

dissociation or a bond formation are not presented in **Figure 2** because those far from the FC region are not very important in photochemistry of benzene. It should be noted that MECIs caused by a bond dissociation or a bond formation were also obtained in the present search. All of the obtained S_0/S_1-MECIs including those involving bond reorganizations are shown in the supporting information, **Table SI1.**

In the previous studies, three low-lying S_0/S_1-MECIs, i.e. I-1, I-2, and I-3, were reported for benzene [9,30,42-44]. All of three S_0/S_1-MECIs were found by GP/SC-AFIR method as shown in **Figure 1**. Additionally, two high energy S_0/S_1-MECIs, I-4 and I-5, were obtained by the present method. As mentioned in the previous paper [22], MECIs found beyond two or more barriers from a given initial structure are not searched in the SC-AFIR method. However, MECIs beyond the second barrier may be found when the barrier is low enough compared to a given γ. I-4 is an MECI beyond I-1 or I-2, and I-5 is also an MECI beyond I-1. The second barrier to reach I-4 and I-5 was higher on the SMF/AFIR function than on the GP/AFIR function, due to the penalty function used in the SMF approach. This would have allowed the GP/SC-AFIR method to overcome the second barrier to reach I-4 and I-5 in the search with the present γ. I-4 was also found by a SMF/SC-AFIR search using a higher collision energy parameter, γ = 200 kJ/mol, in the previous study [30]. The numbers of force calculations required in

the searches by GP/SC-AFIR and SMF/SC-AFIR methods were 5424 and 8582, respectively, where single force calculation includes energy and gradient of the two states. The reduction of the computational cost in the GP/SC-AFIR method was caused by an improved convergence in the optimization step in which the artificial force was applied to induce various geometrical displacements. This is consistent with the previous observation in which the GP method was shown to be more efficient than a penalty function method in optimization of a MECI structure [12].

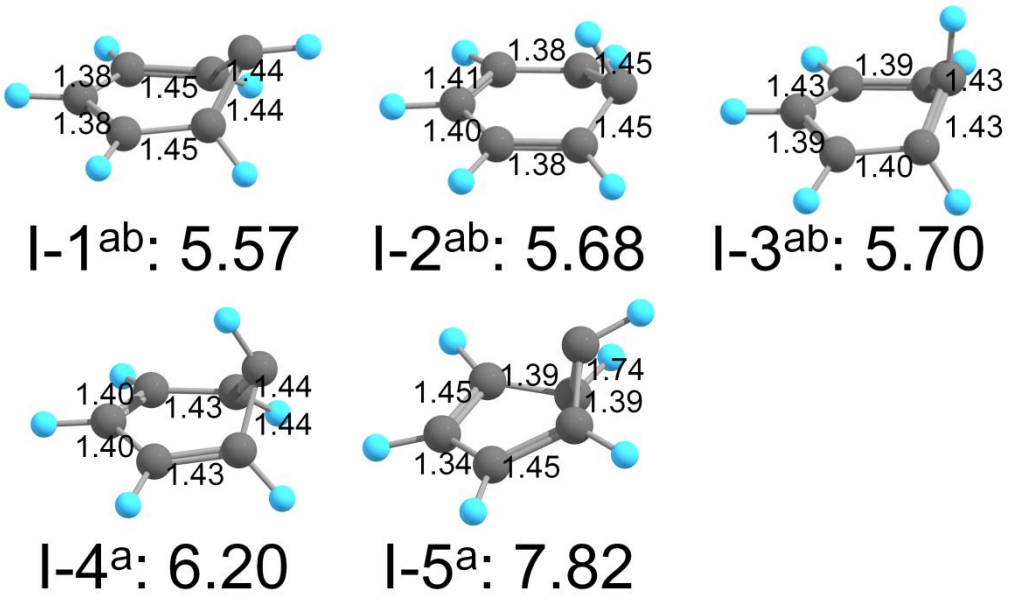

Figure. 1 Molecular geometries of obtained S_0/S_1-MECIs for benzene. S_0/S_1-MECIs obtained by GP/SC-AFIR are indicated by 'a', and those by SMF/SC-AFIR in the previous study [30] are indicated by 'b'. The S_0/S_1-MECI energy is shown relative to the energy at structure of the ground electronic state (S_{0MIN}) in eV. Lengths of carbon-carbon bonds are indicated in Angstrom.

4-2. Naphthalene

S_0/S_1-MECIs of naphthalene are shown in **Figure 2**. S_0/S_1-MECIs obtained by GP/SC-AFIR are indicated by 'a', and those obtained by SMF/SC-AFIR using the same collision energy parameter, γ = 100 kJ/mol, in the previous study are indicated by 'b' [29]. MECIs caused by the molecular motion of a bond dissociation or a bond formation are not shown in Figure 2, where all of the obtained MECIs including those involving

bond reorganizations are shown in the supporting information **Table SI2**. All of the S_0/S_1-MECIs listed in the previous paper [29] were obtained by the present search. As mentioned in the previous paper [22], when there are two or more MECIs in a same direction from the FC point, the SC-AFIR scheme guarantees to find at least one of them. For example, II-3 and II-5 are located in a same direction from the FC point with deformation in the same C-H moiety. Similarly, II-4 and II-6 are located in the same direction. Both SMF/SC-AFIR and GP/SC-AFIR found the lower energy ones, i.e., II-3 and II-4. The higher energy ones, i.e., II-5 and II-6, were also found in the search by the present GP/SC-AFIR method, because of a subtle change in the AFIR-path between SMF/SC-AFIR and GP/SC-AFIR.

The number of force calculations required in the searches by GP/SC-AFIR and SMF/SC-AFIR were 5889 and 7531 [29], respectively, where single force calculation includes energy and gradient of the two states. In the application to naphthalene, the symmetry option of SC-AFIR method was used, since this option was used also in the reference SMF/SC-AFIR calculation [29]. This option was not used in the application to benzene. This is because the total numbers of force calculations are similar between benzene and naphthalene, where the number of force calculations was reduced to 867 in an application of GP/SC-AFIR to benzene when the symmetry option was used.

GP/SC-AFIR was found to be more efficient than SMF/SC-AFIR also in the application to naphthalene.

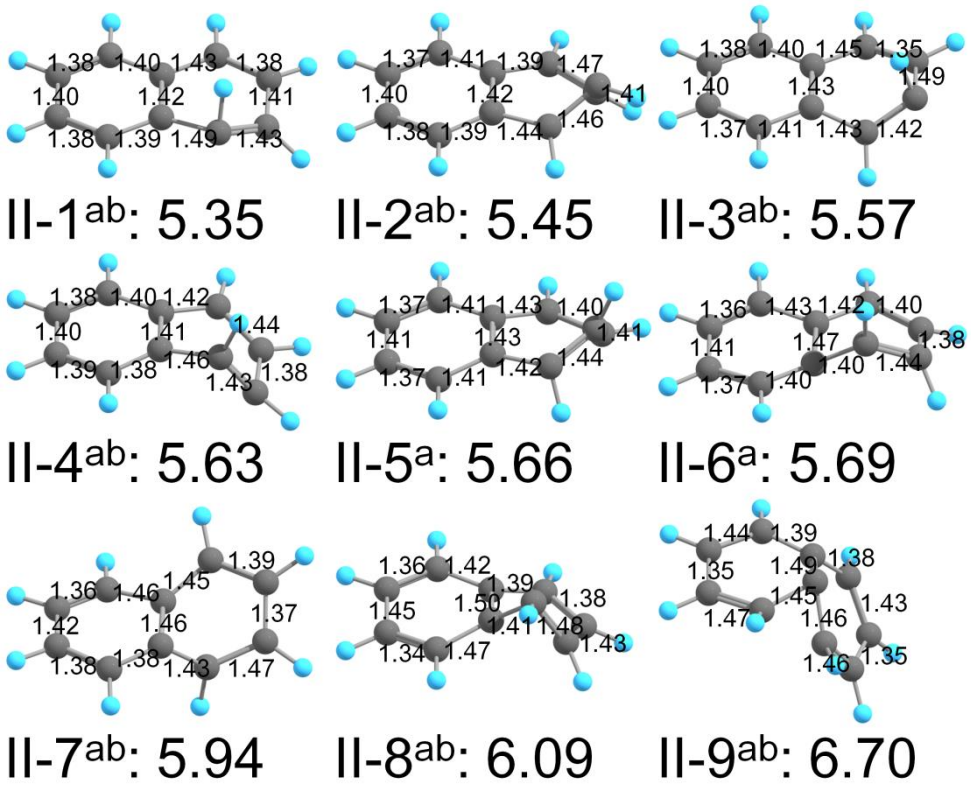

Figure 2. Molecular geometries of obtained S_0/S_1-MECIs for naphthalene. S_0/S_1-MECIs obtained by GP/SC-AFIR are indicated by 'a', and those for SMF/SC-AFIR in the previous study [29] are indicated by 'b'. The S_0/S_1-MECI energy is shown relative to the energy at structure of the ground electronic state (S_{0MIN}) in eV. Lengths of carbon-carbon bonds are indicated in Angstrom.

5. Conclusion

An efficient search method for MECIs has been developed by combining single component artificial force induced reaction (SC-AFIR) method and gradient projection (GP) method. All of the S_0/S_1-MECIs reported in the previous studies were obtained by the present GP/SC-AFIR method. Furthermore, the GP/SC-AFIR method was found to be more efficient than the previous automated MECI search approach, SMF/SC-AFIR. This is because convergence of the GP method is faster than a penalty function method which has been used in the SMF/SC-AFIR method. It is noted that the present approach is also applicable to the search for structures of MESX between two different spin states. The present GP/SC-AFIR method will be one of powerful tools in studies on the mechanism of chemical reactions involving nonadiabatic transition.

Acknowledgements

This work is supported by a grant from Japan Science and Technology Agency with a Core Research for Evolutional Science and Technology (CREST) in the Area of “Establishment of Molecular Technology towards the Creation of New Functions” at Hokkaido University. This research was supported by JST, PRESTO.

References

[1] F. Bernardi, M. Olivucci, M.A. Robb, Potential energy surface crossings in organic photochemistry, Chem. Soc. Rev. 25 (1996) 321.

[2] D.R. Yarkony, Diabolical conical intersections, Rev. Mod. Phys. 68 (1996) 985.

[3] D.R. Yarkony, Conical intersections: Diabolical and often misunderstood, Acc. Chem. Res. 31 (1998) 511.

[4] A.L. Sobolewski, W. Domcke, C. Dedonder-Lardeux, C. Jouvet, Excited-state hydrogen detachment and hydrogen transfer driven by repulsive $^1\pi\sigma^*$ states: A new paradigm for nonradiative decay in aromatic biomolecules, Phys. Chem. Chem. Phys. 4 (2002) 1093.

[5] B.G. Levine, T.J. Martinez, Isomerization through conical intersections, Annu. Rev. Phys. Chem. 58 (2007) 613.

[6] S. Nanbu, T. Ishida, H. Nakamura, Future perspectives of nonadiabatic chemical dynamics, Chem. Sci. 1 (2010) 663.

[7] N. Koga, K. Morokuma, Determination of the Lowest Energy Point on the Crossing Seam between 2 Potential Surfaces Using the Energy Gradient, Chem. Phys. Lett. 119 (1985) 371.

[8] M.R. Manaa, D.R. Yarkony, On the Intersection of 2 Potential-Energy Surfaces of

the Same Symmetry - Systematic Characterization Using a Lagrange Multiplier Constrained Procedure, J. Chem. Phys. 99 (1993) 5251.

[9] M.J. Bearpark, M.A. Robb, H.B. Schlegel, A Direct Method for the Location of the Lowest Energy Point on a Potential Surface Crossing, Chem. Phys. Lett. 223 (1994) 269.

[10] J.M. Anglada, J.M. Bofill, A reduced-restricted-quasi-Newton-Raphson method for locating and optimizing energy crossing points between two potential energy surfaces, J. Comput. Chem. 18 (1997) 992.

[11] C. Ciminelli, G. Granucci, M. Persico, The photoisomerization mechanism of azobenzene: A semiclassical simulation of nonadiabatic dynamics, Chem. Eur. J. 10 (2004) 2327.

[12] T.W. Keal, A. Koslowski, W. Thiel, Comparison of algorithms for conical intersection optimisation using semiempirical methods, Theor. Chem. Acc. 118 (2007) 837.

[13] B.G. Levine, J.D. Coe, T.J. Martinez, Optimizing conical intersections without derivative coupling vectors: Application to multistate multireference second-order perturbation theory (MS-CASPT2), J. Phys. Chem. B 112 (2008) 405.

[14] F. Sicilia, L. Blancafort, M.J. Bearpark, M.A. Robb, New algorithms for optimizing

and linking conical intersection points, J. Chem. Theory Comput. 4 (2008) 257.

[15] S. Maeda, K. Ohno, K. Morokuma, Updated Branching Plane for Finding Conical Intersections without Coupling Derivative Vectors, J. Chem. Theory Comput. 6 (2010) 1538.

[16] F. Sicilia, M.J. Bearpark, L. Blancafort, M.A. Robb, An analytical second-order description of the S_0/S_1 intersection seam: fulvene revisited, Theor. Chem. Acc. 118 (2007) 241.

[17] J.J. Serrano-Pérez, M.J. Bearpark, M.A. Robb, The extended S_1/S_0 conical intersection seam for the photochemical 2+2 cycloaddition of two ethylene molecules, Mol. Phys. 110 (2012) 2493.

[18] J.J. Serrano-Perez et al., How the conical intersection seam controls chemical selectivity in the photocycloaddition of ethylene and benzene, J Org Chem 78 (2013) 1874.

[19] S. Maeda, K. Ohno, K. Morokuma, Automated Global Mapping of Minimal Energy Points on Seams of Crossing by the Anharmonic Downward Distortion Following Method: A Case Study of H_2CO, J. Phys. Chem. A 113 (2009) 1704.

[20] Y. Harabuchi, S. Maeda, T. Taketsugu, N. Minezawa, K. Morokuma, Automated Search for Minimum Energy Conical Intersection Geometries between the Lowest

Two Singlet States S_0/S_1-MECIs by the Spin-Flip TDDFT Method, J. Chem. Theory Comput. 9 (2013) 4116.

[21] S. Maeda, T. Taketsugu, K. Morokuma, Exploring Pathways of Photoaddition Reactions by Artificial Force Induced Reaction Method: A Case Study on the Paterno-Buchi Reaction, Z. Phys. Chem. 227 (2013) 1421.

[22] S. Maeda, Y. Harabuchi, T. Taketsugu, K. Morokuma, Systematic Exploration of Minimum Energy Conical Intersection Structures near the Franck-Condon Region, J. Phys. Chem. A 118 (2014) 12050.

[23] S. Maeda, T. Taketsugu, K. Ohno, K. Morokuma, From Roaming Atoms to Hopping Surfaces: Mapping Out Global Reaction Routes in Photochemistry, J. Am. Chem. Soc. 137 (2015) 3433.

[24] K. Ohno, S. Maeda, A scaled hypersphere search method for the topography of reaction pathways on the potential energy surface, Chem. Phys. Lett. 384 (2004) 277.

[25] S. Maeda, K. Ohno, Global mapping of equilibrium and transition structures on potential energy surfaces by the scaled hypersphere search method: Applications to ab initio surfaces of formaldehyde and propyne molecules, J. Phys. Chem. A 109 (2005) 5742.

[26] K. Ohno, S. Maeda, Global reaction route mapping on potential energy surfaces of formaldehyde, formic acid, and their metal-substituted analogues, J. Phys. Chem. A 110 (2006) 8933.

[27] S. Maeda, K. Morokuma, Finding Reaction Pathways of Type A+B -> X: Toward Systematic Prediction of Reaction Mechanisms, J. Chem. Theory Comput. 7 (2011) 2335.

[28] S. Maeda, T. Taketsugu, K. Morokuma, Exploring transition state structures for intramolecular pathways by the artificial force induced reaction method, J. Comput. Chem. 35 (2014) 166.

[29] S. Maeda, Y. Harabuchi, M. Takagi, T. Taketsugu, K. Morokuma, Artificial Force Induced Reaction (AFIR) Method for Exploring Quantum Chemical Potential Energy Surfaces, Chem. Rec. 16 (2016) 2232.

[30] Y. Harabuchi, T. Taketsugu, S. Maeda, Nonadiabatic Pathways of Furan and Dibenzofuran: What Makes Dibenzofuran Fluorescent?, Chem. Lett. 45 (2016) 940.

[31] Y.H. Shao, M. Head-Gordon, A.I. Krylov, The spin-flip approach within time-dependent density functional theory: Theory and applications to diradicals, J. Chem. Phys. 118 (2003) 4807.

[32] F. Wang, T. Ziegler, Time-dependent density functional theory based on a noncollinear formulation of the exchange-correlation potential, J. Chem. Phys. 121 (2004) 12191.

[33] N. Minezawa, M.S. Gordon, Optimizing Conical Intersections by Spin-Flip Density Functional Theory: Application to Ethylene, J. Phys. Chem. A 113 (2009) 12749.

[34] A.D. Becke, Density-functional exchange-energy approximation with correct asymptotic behavior, Phys Rev A Gen Phys 38 (1988) 3098.

[35] C.T. Lee, W.T. Yang, R.G. Parr, Development of the Colle-Salvetti Correlation-Energy Formula into a Functional of the Electron-Density, Phys. Rev. B 37 (1988) 785.

[36] M. Isegawa, D.G. Truhlar, Valence excitation energies of alkenes, carbonyl compounds, and azabenzenes by time-dependent density functional theory: Linear response of the ground state compared to collinear and noncollinear spin-flip TDDFT with the Tamm-Dancoff approximation, J. Chem. Phys. 138 (2013) 134111.

[37] N. Minezawa, M.S. Gordon, Photoisomerization of Stilbene: A Spin-Flip Density Functional Theory Approach, J. Phys. Chem. A 115 (2011) 7901.

[38] I.N. Ioffe, A.A. Granovsky, Photoisomerization of Stilbene: The Detailed XMCQDPT2 Treatment, J. Chem. Theory Comput. 9 (2013) 4973.

[39] Y. Harabuchi, K. Keipert, F. Zahariev, T. Taketsugu, M.S. Gordon, Dynamics Simulations with Spin-Flip Time-Dependent Density Functional Theory: Photoisomerization and Photocyclization Mechanisms of cis-Stilbene in ππ* States, J. Phys. Chem. A 118 (2014) 11987.

[40] M.W. Schmidt et al., General Atomic and Molecular Electronic-Structure System, J. Comput. Chem. 14 (1993) 1347.

[41] S. Maeda et al., GRRM, a developmental version, Hokkaido University, 2016.

[42] Q. Li et al., A global picture of the S_1/S_0 conical intersection seam of benzene, Chem. Phys. 377 (2010) 60.

[43] L. Blancafort, M.A. Robb, A Valence Bond Description of the Prefulvene Extended Conical Intersection Seam of Benzene, J. Chem. Theory Comput. 8 (2012) 4922.

[44] Y. Harabuchi, T. Taketsugu, S. Maeda, Exploration of minimum energy conical intersection structures of small polycyclic aromatic hydrocarbons: toward an understanding of the size dependence of fluorescence quantum yields, Phys. Chem. Chem. Phys. 17 (2015) 22561.